Inventory of Supplemental Material

Six Figures, Three Tables, Supplemental Experimental Procedures, and Supplemental References

Supplemental Information

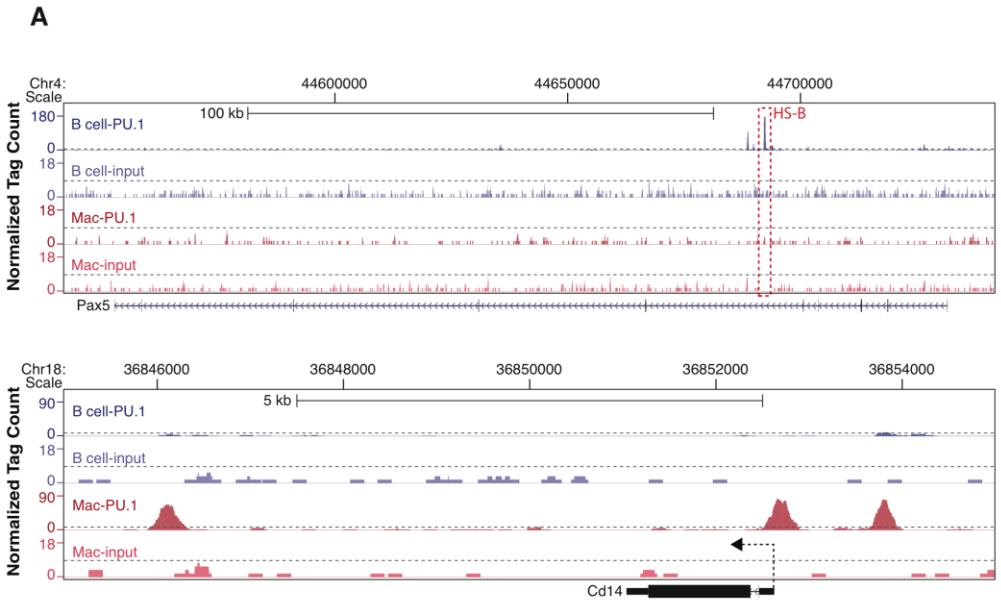

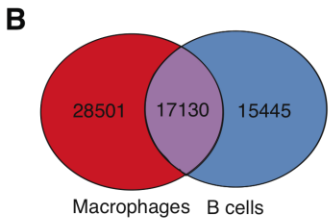

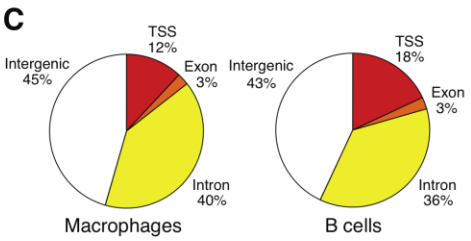

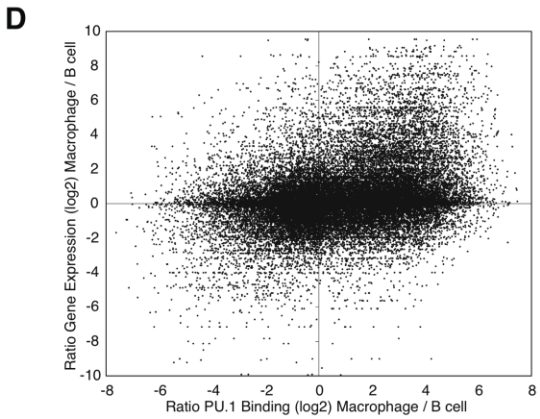

Heinz et al., Figure S1

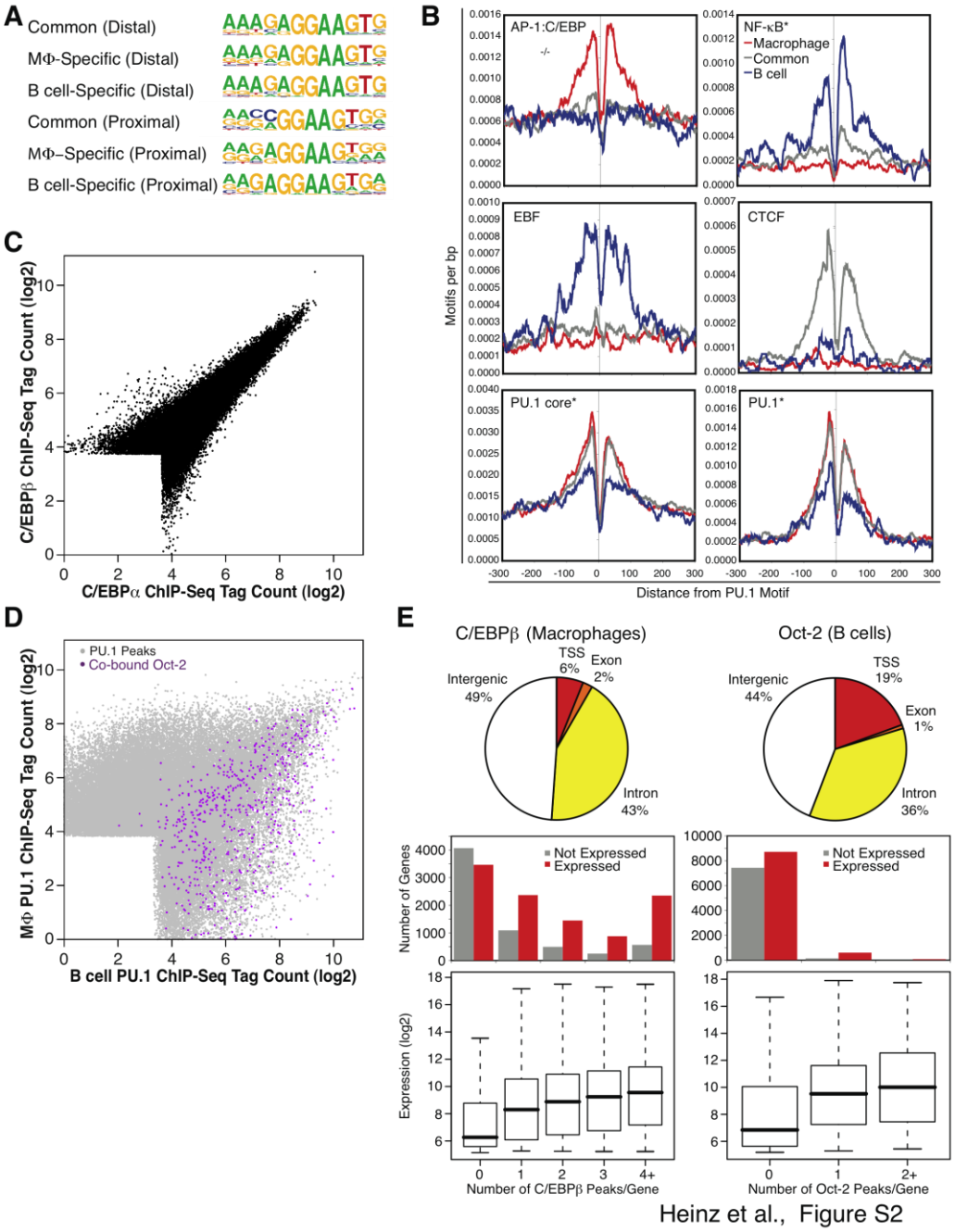

Heinz et al., Figure S2

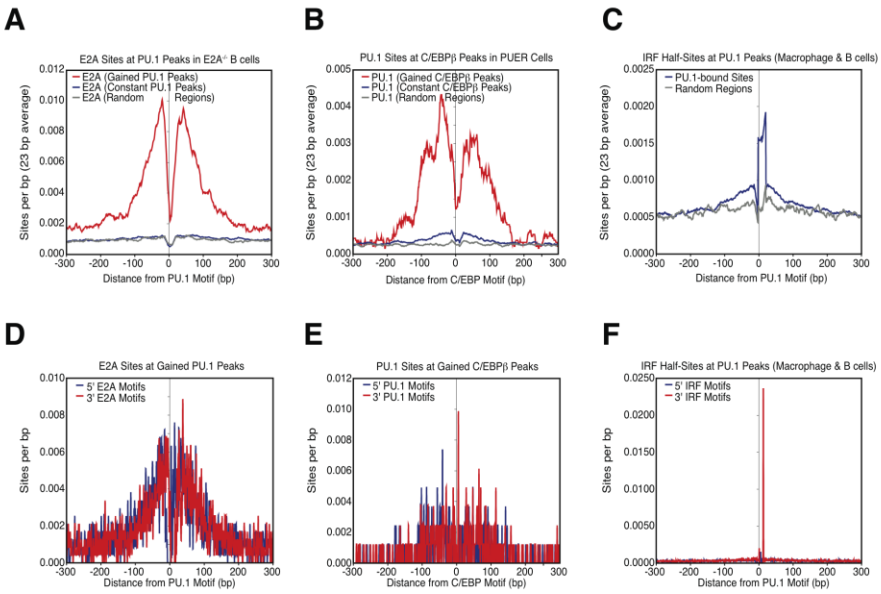

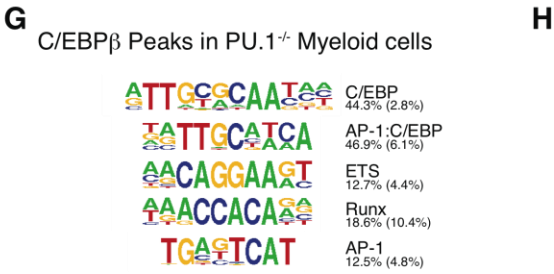

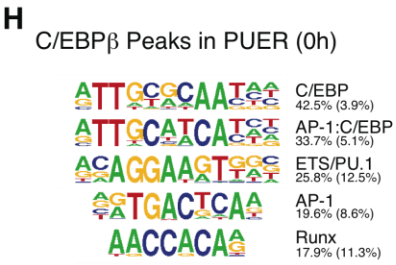

Heinz et al., Figure S3

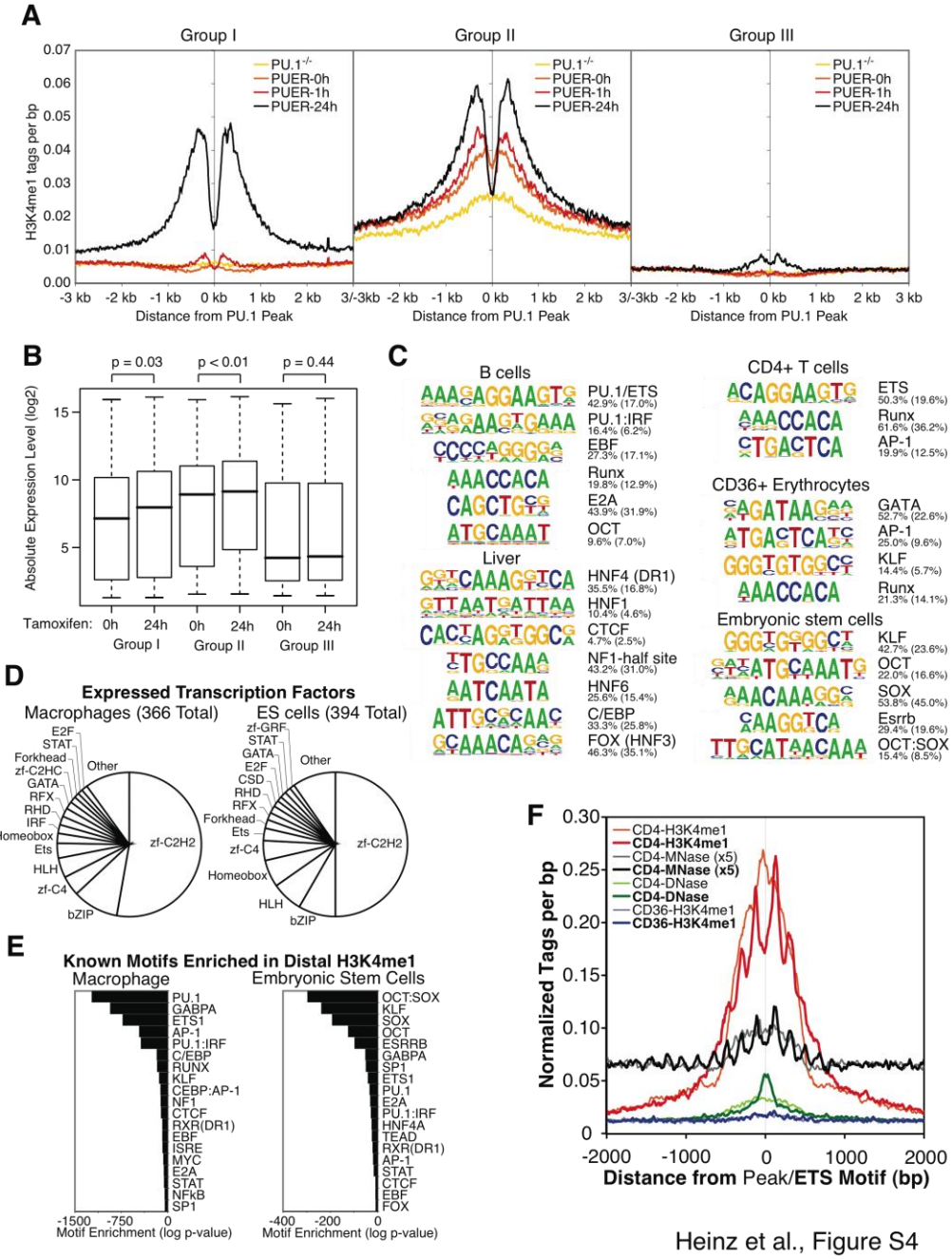

Heinz et al., Figure S4

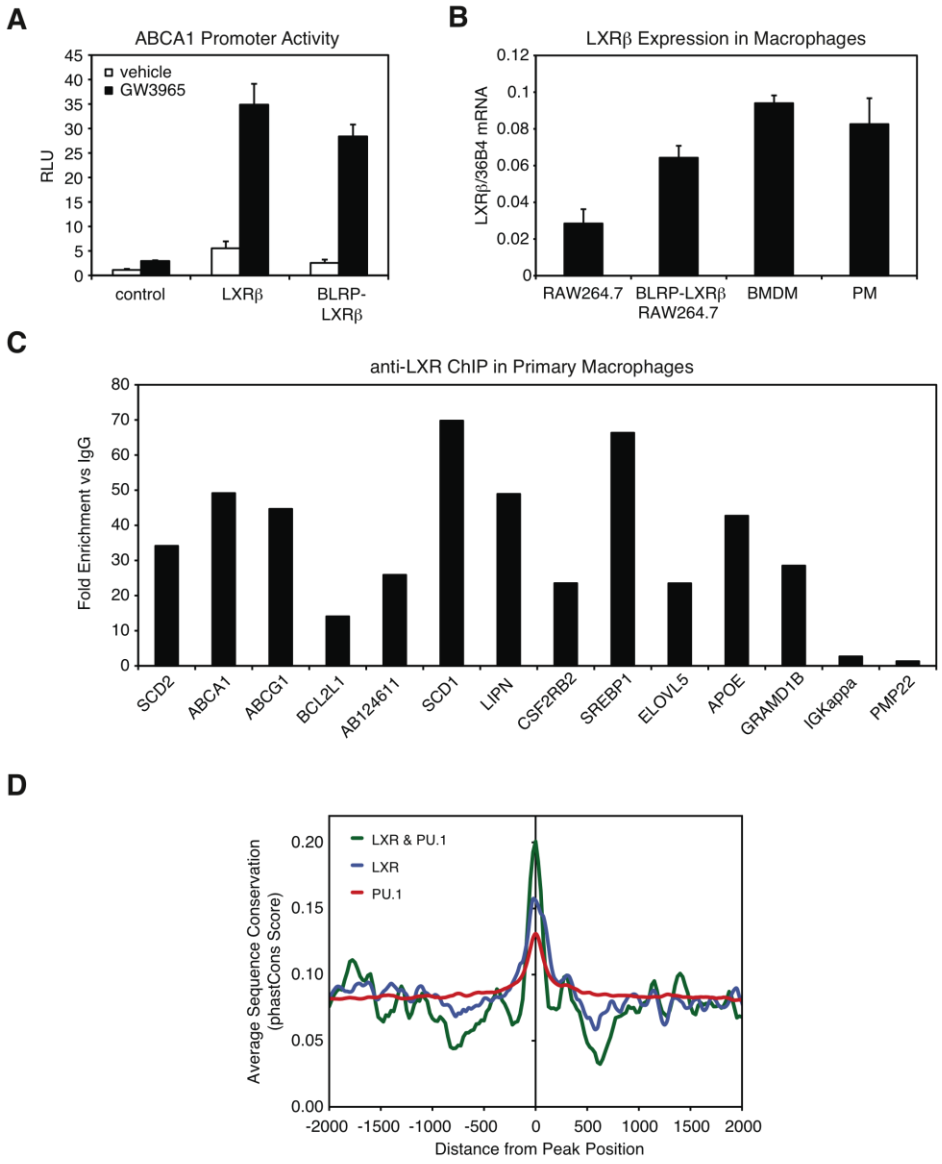

Heinz et al., Figure S5

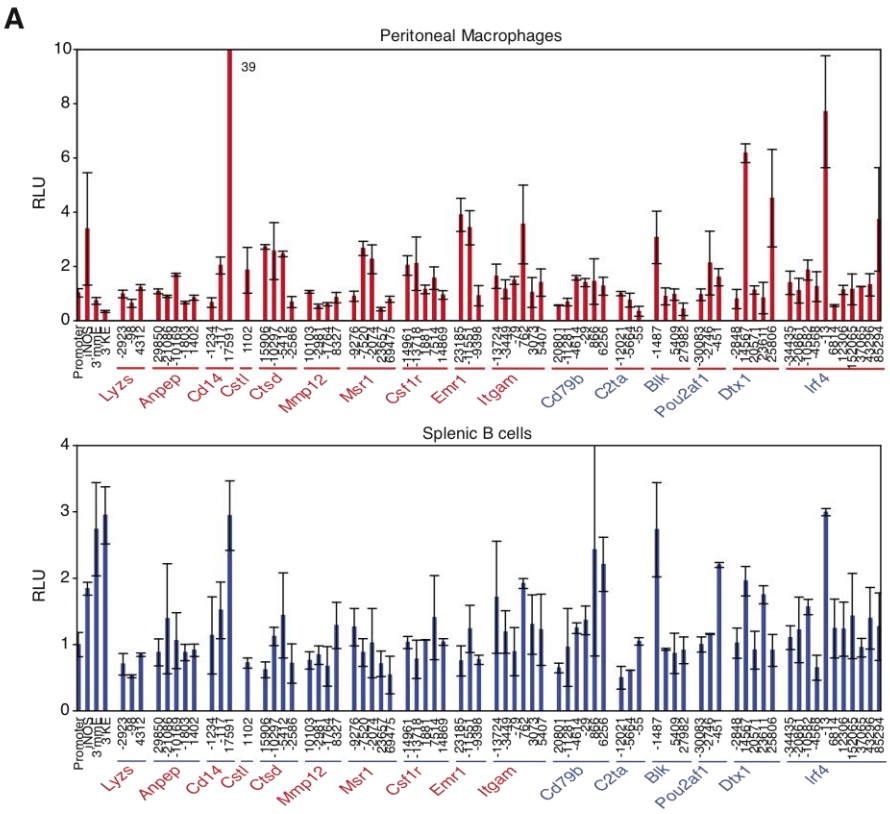

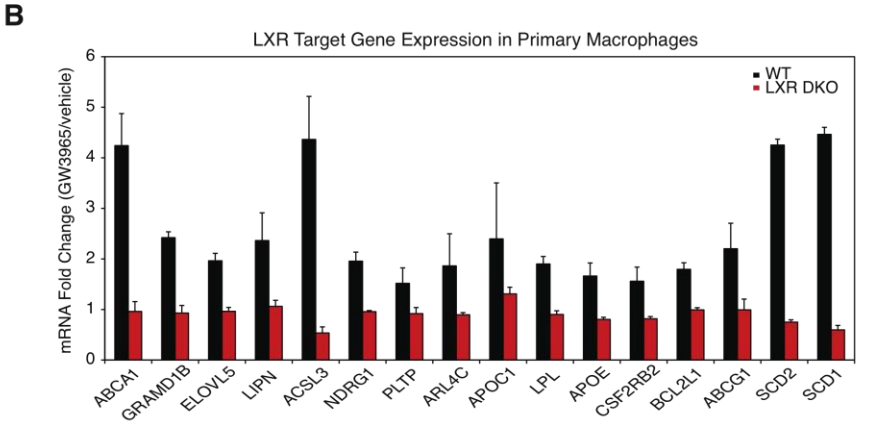

Heinz et al., Figure S6

Supplemental Figure Legends

Figure S1. Characterization of the PU.1 ChIP-Seq experiment in mouse macrophages and B cells - Related to Figure 1

(A) UCSC Genome Browser images of the PU.1 ChIP-Seq data and the associated input sequencing data at the B cell-specific Pax5 gene and the macrophage-specific CD14 gene. The DNase I-hypersensitive site B (HS-B) of the Pax5 intronic enhancer in intron 5 (Decker et al., 2009) and the CD14 promoter (Pan et al., 1999) are indicated. All tag count numbers were normalized to 10^7 sequence tags. Input signal, and in the case of the Pax5 locus the PU.1 signal in macrophages, is shown 10-fold magnified.

(B) Distribution of independently identified PU.1 ChIP-Seq peaks in macrophages and B cells. Venn diagram of PU.1 peaks identified using a false discovery threshold of 0.1%. Peaks were considered co-bound in both macrophages and B cells if peaks from both cell types were found within 100 bp of each other.

(C) Genomic annotation of PU.1 peak positions in macrophages and B cells, respectively. Peaks found within 500 bp of the TSS were annotated as “TSS”.

(D) Gene expression and PU.1 binding at vicinal sites are correlated. Scatter plot showing a random subset of the total data presented in Figure 1F. The data for 32000 randomly chosen PU.1 peak positions defined in macrophages and/or B cells are shown. For each peak position, the ratio of gene expression values of the gene with the closest TSS as determined by cDNA array hybridisation in both cell types were plotted against the PU.1 peak tag count ratio.

Figure S2. Characterization of PU.1-associated motifs - Related to Figure 2

(A) Top motifs of 12 bp length identified by *de novo* motif discovery at PU.1 peak positions occupied specifically in macrophages or B cells, and peaks common to both cell types in proximal (within ± 500 bp from TSS) or distal (> 500 bp from TSS) regions.

(B) Context-specific frequencies of AP1:C/EBP, NF-κB, EBF, CTCF, PU.1-core and PU.1 motifs in the vicinity of the central PU.1 motif found in PU.1 binding sites. Motif frequencies are centred on distal macrophage-specific PU.1 sites (red), distal B cell-specific PU.1 binding sites (blue), and common distal PU.1 binding sites (grey) (> 500 bp from the nearest TSS). Motif frequencies are shown as a moving average of 23 bp. *Motif frequencies at 0 bp were artificially set to zero for PU.1, PU.1-core, and NFκB (i.e. GGAAttcc) to avoid cross-recognition of the PU.1 motif defined at that position.

(C) Highly overlapping C/EBPα and C/EBPβ binding patterns in macrophages. C/EBPα and C/EBPβ-bound sites are represented by the logarithmic normalized C/EBPα and C/EBPβ ChIP-Seq tag count within 200 bp of each genomic peak position identified in either experiment. Tag counts were normalized to the total tag count for each experiment. To enable visualization of low tag number-containing sites, random jitter (0-1 tags) was added.

(D) Scatter plot of PU.1 ChIP-Seq peaks in macrophages and B cells, represented by logarithmic, jittered, normalized PU.1 ChIP-Seq tag counts (Same as Fig. 1C). Sites co-bound by Oct-2, with an Oct-2 peak within 100 bp of the PU.1 peak position, are coloured purple.

(E) Genomic annotation of peaks found in C/EBPβ and Oct-2 peaks, respectively. Number of genes that contain the specified number of C/EBPβ peaks or Oct-2 peaks, respectively. Box plots depicting the distribution of gene

expression values for genes with the specified number of C/EBPβ or Oct-2 binding sites, respectively, near their promoters.

Figure S3. Distances between the motifs of factors that are co-dependent for binding suggest a collaborative interaction model – Related to Figure 3

(A) Frequency of E2A motifs near PU.1 motifs in PU.1 peaks dependent on E2A for binding in pre-pro-B cells. Motif frequency reported as a 23 bp moving average.

(B) Frequency of PU.1 motifs near C/EBP motifs in C/EBPβ peaks dependent on PU.1 for binding in PUER cells. Motif frequency is reported as a 23 bp moving average.

(C) Frequency of IRF motifs near PU.1 peaks in all PU.1 peaks found in macrophages and B cells. Motif frequency reported as a 23 bp moving average.

(D) Frequency of E2A motifs near PU.1 motifs in PU.1 peaks dependent on E2A for binding in B cells. Motif frequency reported at single base pair resolution.

(E) Frequency of PU.1 motifs near C/EBP motifs in C/EBPβ peaks dependent on PU.1 for binding in PUER cells. Motif frequency reported at single base pair resolution.

(F) Frequency of IRF motifs (GTGAAACT) near PU.1 peaks in all PU.1 peaks found in macrophages and B cells. Motif frequency reported at single base pair resolution. Specific spacing between PU.1 and IRF motifs is indicative of the known ternary complex formed between the proteins, while the non-specific spacing within the length of a nucleosome seen for E2A-PU.1 and PU.1-C/EBP

suggest a collaborative mode of interaction between transcription factors where the combined affinity of the factors to DNA is capable of displacing nucleosomes.

(G) Top motifs identified in 22,641 total C/EBPβ-bound regions in PU.1$^{-/-}$ myeloid cells using *de novo* motif discovery. The fraction of peaks containing at least one instance of each motif within 100 bp of the peak center is given to the right of the motif with the expected frequency of the motif in random regions given in parentheses.

(H) Top motifs identified in 46,628 total C/EBPβ-bound regions in PUER cells in the absence of tamoxifen using *de novo* motif discovery. The fraction of peaks containing at least one instance of each motif within 100 bp of the peak center is given to the right of the motif with the expected frequency of the motif in random regions given in parentheses.

Figure S4 Lineage-determining transcription factors are associated with the cell type-specific H3K4me1 pattern – Related to Figure 4

(A) Cumulative levels of H3K4me1 are shown around PU.1 peaks from groups I, II, and III in PU.1$^{-/-}$ and PUER cells.

(B) Distribution of gene expression values before and after 24 hours of tamoxifen treatment in PUER cells of genes associated with PU.1 peaks from Groups I, II and III. Only Groups I and II exhibited a significant increase in their gene expression distributions from 0 and 24 hours (non-parametric Mann-Whitney test).

(C) H3K4me1-associated motifs identified using *de novo* motif analysis in B cells, human CD4^{+} T cells, human CD36^{+} erythrocytes, mouse liver, and mouse

embryonic stem cells. Sequence logos represent the most enriched sequence elements located within 500 bp of focal H3K4me1-marked regions. (Data from Barski, 2008; Cui, 2009; Wederell, 2008; Mikkelsen, 2007; Meissner, 2008). The fraction of peaks containing at least one instance of each motif within 500 bp of the center of the H3K4me1-marked region is given to the right of the motif with the expected frequency of the motif in random regions given in parentheses.

(D) Total number of transcription factors expressed in macrophages and ES cells. Transcription factors accessions categorized by their Pfam DNA binding domains (Wilson et al., 2008) were used to annotate the mouse gene expression data from BioGPS (Wu et al., 2009)

(E) Top 20 most-highly enriched known transcription factor motifs in macrophages and ES cell distal H3K4me1 marked regions.

(F) Profiles of H3K4me1-modified and total nucleosomes revealed by mononucleosomal sequencing and DNase I hypersensitivity at 2213 H3K4me1-marked regions in $CD4^+$ T cells, aligned on the primarily enriched ETS motif (in bold) (Data from Barski, 2007; Boyle, 2008; Schones, 2008).

Figure S5. Functional validation of biotin-tagged LXRβ and characterization and confirmation of the LXRβ ChIP-Seq data – Related to Figure 5

(A) Biotin-tagged LXRβ demonstrates ligand-dependent activation function. BIRA-RAW264.7 cells were co-transfected with ABCA1 promoter reporter

plasmid and either control vector, LXRβ, or BLRP-LXRβ for 24 hr then treated with vehicle (DMSO) or 1 μM GW3965 for 24 hr. Luciferase assays were performed and values for vehicle- (white bars) and GW3965-treated (black bars) samples are given as relative light units (RLU) after normalization to an internal β-galactosidase control. Results are expressed as the average of three independent experiments ($P<0.05$). Error bars are given as + SEM (two-tailed Student's *t* test, n=3).

(B) Expression level of LXRβ in the BLRP-LXRβ RAW264.7 cell line is similar to that in primary macrophages. Quantitative RT-PCR analysis was used to determine relative expression levels of LXRβ (normalized to 36B4) in RAW264.7 cells, BLRP-LXRβ RAW264.7 cells, bone marrow derived macrophages, and thioglycollate-elicited peritoneal macrophages. Gene expression was analyzed in independent experiments and the averages of duplicates of representative samples are indicated with error bars as + SEM (two-tailed Student's *t* test, n=2).

(C) BLRP-LXRβ ChIP-Seq defined binding sites vicinal to GW3965-responsive genes are bound by LXRα/β in primary macrophages. ChIP-qPCR analysis of LXR binding at indicated loci was performed on chromatin isolated from C57BL/6 bone marrow-derived macrophages using a cocktail of antibodies directed against LXRα and LXRβ. Values are represented as fold enrichment over background (IgG-ChIP). The results are representative of two independent experiments.

(D) Average Phastcons Score plotted as a function of distance from regions bound by LXRβ, PU.1, or peaks co-bound by both factors.

Figure S6. Enhancer reporter assays of genomic PU.1-bound regions and characterization of LXR-dependent target genes in primary cells – Related to Figure 6

(A) Regions flanking PU.1 peaks in the vicinity of macrophage- (red gene names) or B cell-specific (blue gene names) genes were tested for enhancer activity in transient transfections of **a,** primary thioglycolate-elicited peritoneal macrophages or **b,** LPS-activated resting splenic B cells. Locus names are red if the gene is preferentially expressed in macrophages, and blue if preferentially expressed in B cells. Results are averages of at least three independent experiments, normalized for the activity of the reporter construct containing the minimal Vk IIB promoter and lacking an enhancer insert, with transfections performed in duplicates. The macrophage-specific iNos enhancer and the B cell-specific Igκ 3' and Igμ 3' enhancers were used as positive controls, the promoter-less reporter as negative control.

(B) Quantitative RT-PCR analysis of gene expression of representative GW3965-responsive genes was performed comparing wild type (WT) versus LXR$\alpha/\beta^{-/-}$ bone marrow derived macrophages treated with either vehicle (DMSO) or 1 μM GW3965 for 24 hr. Relative expression levels (normalized to 36B4) displayed as fold change of GW3965 versus vehicle, with values for WT and LXR$\alpha/\beta^{-/-}$ macrophages indicated by black and red bars respectively. Gene expression was analyzed in independent experiments and the averages of duplicates of representative samples are indicated with error bars as SEM (two-tailed Student's *t* test, n=3).

Table S1. Summary of ChIP-Seq data used in this study.

(Primary sequencing data is available at GEO, accession no. GSE21512)

(A) High-throughput sequencing data generated in this study

Cell Type (Treatment)	Target Protein	Total Uniquely Mapped Tags (mm8)	Total Peaks Identified * filtered for peaks >3kb from nearest TSS
Macrophage	PU.1	5,293,530	45,631
Macrophage	C/EBPα	7,060,000	35,653
Macrophage	C/EBPβ	6,469,879	41,527
Macrophage	H3K4me1	8,082,290	19,410*
Macrophage	H3K4me3	6,885,937	13,945
Macrophage	None (input)	5,289,281	73
B cell	PU.1	8,861,792	32,575
B cell	Oct2	5,304,724	1,191
B cell	H3K4me1	8,874,085	17,809*
B cell	H3K4me3	5,353,210	13,322
B cell	None (input)	5,401,971	159
E2A$^{-/-}$ pre-pro-B cell	PU.1	5,091,724	44,609
EBF$^{-/-}$pre-pro-B cell	PU.1	3,058,912	36,908
RAG1$^{-/-}$ pro-B cell	PU.1	6,314,038	17,210
E2A$^{-/-}$ pre-pro-B cell, transduced with bHLH-ER, 6 h tamoxifen	PU.1	4,731,840	41,456
E2A$^{-/-}$ pre-pro-B cell, transduced with wt E47-ER, 6 h tamoxifen	PU.1	3,614,551	39,256
PU.1$^{-/-}$ myeloid cell	PU.1	4,627,336	18
PUER	PU.1	2,051,877	8,144
PUER, 1 h Tamoxifen	PU.1	2,542,888	37,909
PUER, 6 h Tamoxifen	PU.1	3,479,495	54,059
PUER, 24 h Tamoxifen	PU.1	3,405,292	43,012
PUER, 48 h Tamoxifen	PU.1	4,140,503	48,769
PU.1$^{-/-}$ myeloid cell	C/EBPβ	4,222,205	22,641
PUER	C/EBPβ	4,658,691	46,628
PUER, 1h Tamoxifen	C/EBPβ	3,780,006	39,131
PUER, 6 h Tamoxifen	C/EBPβ	4,403,415	40,280
PUER, 24 h Tamoxifen	C/EBPβ	4,615,227	41,686
PUER, 48 h Tamoxifen	C/EBPβ	5,002,872	43,081
PU.1$^{-/-}$ myeloid cells	H3K4me1	7,110,724	22,103*
PUER	H3K4me1	8,115,864	19,993*
PUER, 1 h Tamoxifen	H3K4me1	7,272,352	19,603*
PUER, 24 h Tamoxifen	H3K4me1	5,770,918	20,280*
PUER	Nucleosomes	25,034,876	NA
PUER, 1 h Tamoxifen	Nucleosomes	29,902,469	NA
RAW264.7, 1 h GW3965	BLRP-LXRβ	12,497,324	664
RAW264.7, 1 h GW3965	BirA-control	12,669,507	1,010
BMDM	PU.1	13,022,713	83,447
BMDM LXRα/β$^{-/-}$	PU.1	13,754,386	83,512
BMDM	H3K4me1	14,214,530	21,327*
BMDM LXRα/β$^{-/-}$	H3K4me1	14,905,848	19,363*

(B) Published data used in this study

Cell Type (Treatment)	Target Protein	Total Uniquely Mapped Tags (mm8/hg18)	Total Peaks Identified * filtered for peaks >3kb from nearest TSS
ES cells (Meissner, 2008)	H3K4me1	5,974,589	9,972*
ES cells (Mikkelsen, 2007)	H3K4me3	8,850,116	21,602
ES cells (Mikkelsen, 2007)	Input	715,231	46
Liver (Wederell, 2008)	H3K4me1	24,525,576	24,044*
Liver (Wederell, 2008)	H3K4me3	2,817,653	16,202
$CD36^+$ Erythrocytes (Cui, 2009)	H3K4me1	8,407,012	22,580*
$CD36^+$ Erythrocytes (Cui, 2009)	H3K4me3	2,031,243	13,318
$CD4^+$ T cells (Barski, 2007)	H3K4me1	11,322,526	17,583*
$CD4^+$ T cells (Barski, 2007)	H3K4me3	16,845,478	24,694
$CD4^+$ T cells (Schones, 2008)	Nucleosomes	115,702,344	NA
$CD4^+$ T cells (Boyle, 2008)	DNase I digest	22,451,212	33,343
BMDM (Ghisletti, 2010)	p300	14,207,429	13,241
BMDM (Ghisletti, 2010)	Input	7,318,448	185

Table S2. Frequency of predicted motifs in PU.1-bound regions – Related to Figure 2A

Motif	Common (Distal)	Common (Proximal)	Macrophage-Specific (Distal)	Macrophage-Specific (Proximal)	B cell Specific (Distal)	B cell Specific (Proximal)	100k Random Regions
PU.1 (ETS)	53.0%	19.3%	53.5%	38.9%	45.1%	29.7%	5.0%
PU.1-core (ETS)	79.5%	69.4%	82.4%	77.7%	74.1%	63.0%	20.8%
GABP (ETS)	52.0%	46.8%	49.5%	44.0%	46.5%	40.6%	5.4%
PU1-IRF	8.9%	2.1%	5.6%	3.6%	17.3%	6.9%	1.0%
CTCF	7.2%	3.0%	1.0%	1.7%	2.1%	1.7%	0.9%
SP1	7.8%	40.5%	5.0%	21.0%	7.1%	30.0%	2.9%
NFY	5.3%	18.5%	4.5%	7.4%	4.5%	10.2%	5.2%
CRE	4.1%	14.9%	3.8%	4.5%	4.3%	12.2%	1.9%
NRF	0.9%	11.8%	0.2%	1.9%	0.3%	2.0%	0.2%
GFY	0.7%	7.3%	0.3%	1.7%	0.3%	1.7%	0.5%
E2A	15.8%	14.8%	7.1%	8.5%	34.7%	37.0%	20.6%
EBF	4.2%	5.1%	2.8%	6.2%	8.8%	12.5%	2.6%
OCT	2.6%	1.1%	1.2%	1.3%	7.7%	5.3%	2.7%
NFkB	4.1%	4.0%	2.7%	2.6%	8.2%	11.2%	1.9%
C/EBP	12.2%	6.2%	22.9%	16.3%	8.7%	7.3%	13.7%
AP1	9.3%	3.3%	20.9%	9.5%	6.3%	3.3%	6.4%
AP1:C/EBP	14.0%	6.2%	21.8%	14.7%	12.8%	8.9%	13.6%

Table S3: Percentage of gained, lost or unchanged PU.1 peaks in EBF$^{-/-}$, RAG1$^{-/-}$, and immature B cells relative to E2A$^{-/-}$ CLP that contain the respective motif – Related to Figure 3A

Peaks	Number of Peaks	RUNX	E2A	EBF	OCT	NF-κB
Gained in EBF$^{-/-}$	3760	27.2%	33.5%	4.0%	1.4%	2.3%
Lost in EBF$^{-/-}$	2996	12.6%	15.1%	4.6%	2.1%	6.2%
Constant in EBF$^{-/-}$	38272	18.4%	21.0%	4.0%	1.7%	3.3%
Gained in Rag1$^{-/-}$	2479	14.8%	29.9%	14.2%	8.4%	2.0%
Lost in Rag1$^{-/-}$	25377	19.8%	19.9%	3.6%	1.2%	4.4%
Constant in Rag1$^{-/-}$	11902	15.0%	21.0%	4.7%	3.1%	2.3%
Gained in B cells	9504	12.8%	23.4%	7.6%	6.4%	6.7%
Lost in B cells	22082	20.0%	19.4%	3.5%	1.2%	2.9%
Constant in B cells	17019	15.4%	20.9%	4.5%	2.2%	4.2%
Random	100000	10.7%	17.1%	3.4%	2.7%	1.9%

Supplemental Experimental Procedures

Cell isolation and culture

Primary cells were isolated from male 6-8 week-old C57Bl/6 mice (Charles River Laboratories, Wilmington, MA, USA).

Peritoneal macrophages were harvested by peritoneal lavage with 10 ml ice-cold PBS 3 days after peritoneal injection of 3 ml 3 % thioglycollate. Peritoneal cells were washed once with PBS, and seeded in 10% fetal calf serum (FCS)/DMEM containing 100 U penicillin/streptomycin in tissue culture-treated petri dishes overnight. Non-adherent cells were washed off with room temperature PBS. BMDM were generated from C57BL/6 mice as previously described (Valledor et al., 2004).

Splenic B cells were isolated by magnetic depletion of CD43- and CD11b-expressing cells (Miltenyi, Bergisch Gladbach, Germany). B cell preparations were over 96% pure as assessed by flow cytometry for B220 expression.

Pro-B cells were cultured as described previously (Sayegh et al., 2005) with slight modifications. Pro-B cells were isolated from femoral bone marrow of Rag1 knockout mice by positive enrichment of $B220^{+}$ cells using magnetic separation (Miltenyi) and expanded for 10 d in Opti-MEM medium containing 10% FCS, 2x penicillin/streptomycin/glutamine, and 50 μM β-mercaptoethanol supplemented with 1:100 IL-7 and 1:500 SCF. $E2A^{-/-}$and $EBF^{-/-}$ pre-pro-B cells were cultured as described previously (Ikawa, 2004). $PU.1^{-/-}$ and PUER cells were propagated and the PU.1-ER fusion protein was activated with 100 nM 4-hydroxy-tamoxifen as described (Walsh, 2002).

The murine RAW 264.7 macrophage cell line was obtained from the American Type Culture Collection (ATCC).

Expression Array Profiling

Total RNA from thioglycollate-elicited macrophages (pooled from 3 mice) and splenic B cells (pooled from 2 mice) was purified using RNeasy columns (Qiagen). Samples (250 ng RNA) were amplified and labeled using the Quick AMP Labeling kit (Agilent) and hybridized to 44K Whole Mouse Genome Oligo Microarrays (Agilent) according to the manufacturer's instructions. Slide image data was quantified the using Agilent's Feature Extraction software. Two biological replicates were performed for each cell type.

Retroviral transduction

E47-ER-Tac and bHLH-ER-Tac retroviral constructs have been described (Sayegh, 2003). Virus was generated by transfection of the constructs and packaging vector into 293T cell line using calcium phosphate precipitation. E2A-deficient hematopoietic progenitor cells were transduced as described previously (Quong, 1999). E47-ER and bHLH-ER were activated for 6 hr with 1 μM 4-hydroxy-tamoxifen and transduced cells were isolated by magnetic selection (Miltenyi) for the bi-cistronically co-expressed human CD25 (TAC antigen).

Chromatin immunoprecipitation (ChIP)

ChIP was performed as described previously (Metivier, 2003), with modifications. Briefly, 10-20 Mio cells were crosslinked in 1% Formaldehyde/PBS for 10 minutes at room temperature. The reaction was quenched by adding glycine to a final concentration of 125 mM, and the cells were centrifuged immediately (5 min, 700x g, 4°C) and washed twice with ice-cold PBS. Cells were resuspended in swelling buffer (10 mM HEPES/KOH pH7.9, 85 mM KCl, 1 mM EDTA, 0.5% IGEPAL CA-630, 1x protease inhibitor cocktail (Roche), 1 mM PMSF) for 5 minutes. Cells were spun down and resuspended in 500 μl lysis buffer (50 mM Tris/HCl pH 7.4@20°C, 1% SDS, 0.5% Empigen BB, 10 mM EDTA, 1x protease inhibitor cocktail (Roche), 1 mM PMSF)) and chromatin was sheared to an average DNA size of 300-400 bp by administering 6 pulses of 10 seconds duration at 12 W power output with 30 seconds pause on wet ice using a Misonix 3000 sonicator. The lysate was cleared by centrifugation (5 min, 16000 x g, 4°C), and 500 μl supernatant was diluted 2.5-fold with 750 μl dilution buffer (20 mM Tris/HCl pH 7.4@20°C, 100 mM NaCl, 0.5% Triton X-100, 2 mM EDTA, 1x protease inhibitor cocktail (Roche)). The diluted lysate was pre-cleared by rotating for 2 h at 4°C

with 120 µl 50% CL-4B sepharose slurry (Pharmacia, Uppsala, Sweden; Before use, up to 250 µl CL-4B sepharose were washed twice with 1 ml TE buffer, blocked for > 30 min at room temperature with 0.5% BSA and 20 µg/ml glycogen in 1 ml TE buffer, washed twice with TE and brought up to the original volume with TE). The beads were discarded, and 1% of the supernatant were kept as ChIP input. The protein of interest was immunoprecipitated by rotating the supernatant with 2.5 µg antibody overnight at 4°C, then adding 50 µl blocked protein A-sepharose CL-4B (GE Healthcare, Piscataway, NJ, USA; protein A-sepharose CL-4B was blocked as CL-4B above, except that it was rotated overnight at 4°C) and rotating the sample for an additional 1 ½ to 2 h at 4°C. The beads were pelleted (2 min, 1000 x g, 4°C), the supernatant discarded, and the beads were transferred in 400 µl wash buffer I (WB I) (20 mM Tris/HCl pH 7.4@20°C, 150 mM NaCl, 0.1% SDS, 1% Triton X-100, 2 mM EDTA) into 0.45 µm filter cartridges (Ultrafree MC, Millipore, Billerica, MA, USA), spun dry (1 min, 2200 x g, 4°C), washed one more time with WB I (20 mM Tris/HCl pH 7.4@20°C, 150 mM NaCl, 0.1% SDS, 1% Triton X-100, 2 mM EDTA), and twice each with WB II (20 mM Tris/HCl pH 7.4@20°C, 500 mM NaCl, 1% Triton X-100, 2 mM EDTA), WB III (10 mM Tris/HCl pH 7.4@20°C, 250 mM LiCl, 1% IGEPAL CA-630, 1% Na-deoxycholate, 1 mM EDTA), and TE. Immunoprecipitated chromatin was eluted twice with 100 µl elution buffer each (100 mM $NaHCO_3$, 1% SDS) into fresh tubes for 20 min and 10 min, respectively, eluates were pooled, the Na^+ concentration was adjusted to 300 mM with 5 M NaCl and crosslinks were reversed overnight at 65°C in a hybridization oven. The samples were sequentially incubated at 37°C for 2 h each with 0.33 mg/ml RNase A and 0.5 mg/ml proteinase K. The DNA was isolated using the

QiaQuick PCR purification kit (Qiagen, Hilden, Germany) according to the manufacturer's instructions.

Antibodies against PU.1 (sc-352), C/EBPα (sc-61), C/EBPβ (sc-150), Oct2 (sc-233) and pan-LXR (sc-1000) were purchased from Santa Cruz Biotech (Santa Cruz, CA, USA), antibodies against H3K4me1 (ab8895) and H3K4me3 (ab8580) were from Abcam (Cambridge, MA, USA), antibodies against LXRβ (PP-K8917-00) were from Perseus Proteomics (Tokyo, Japan). Primer sequences for ChIP-qPCR analysis of LXR target loci are given below.

MNase-seq

Micrococcal nuclease digest and deep sequencing (MNase-seq) were essentially performed as described (Schones, 2008). Briefly, $5x10^6$ PUER cells were either treated with 100 nM tamoxifen or vehicle. Cells were washed once with PBS at room temperature, permeabilized by resuspending in 200 µl MNase buffer (50 mM Tris/HCl pH 7.6, 1 mM $CaCl_2$, 0.2 % IGEPAL CA-630 (Sigma), 1x protease inhibitor cocktail without EDTA (Sigma), 1 mM PMSF), and immediately digested with 30 U MNase (Worthington Biochemicals) for 5 minutes at 24°C. The reaction was stopped by adding 50 µl 5x SDS-Stop buffer (10 mM Tris/HCl pH 7.6, 5 mM EDTA, 50 mM EGTA, 5% SDS) and the samples were digested with 0.33 mg/ml RNase for 45 minutes at 24°C, then overnight with 0.33 mg/ml proteinase K at 37°C. The reaction was supplemented with 25 µl 3 M NaOAc pH 5.5, extracted once with an equal volume phenol/chloroform (1:1), once with half a volume chloroform. DNA was precipitated overnight at -20°C after adding 750 µl 100% ethanol, washed twice with 85% ethanol, air-dried and dissolved in TE buffer. Two microgram DNA each were run on a 2% agarose/TBE (SeaKem LE) gel, and mononucleosomal DNA (about 85% were mononucleosomal,

12.5% dinucleosomal ass assessed by densitometry of the gel image) was size-selected (135-155 bp) and gel-extracted (QiaQuick, Qiagen). MNase fragments were sequenced without prior DNA amplification for 36 cycles on an Illumina GA II following end-polishing, A-overhang addition, ligation of single-end read direct sequencing linkers (A_adapter_t: 5'-AATGATACGGCGACCACCGAGATCTACACTCTTTCCCTACACGACGCTCTTCCGATC*T-3', A_SRadapter_b: 5'-p-GATCGGAAGAGCTCGTATGCCGTCTTCTGCTTG-3'; *:phosphorothioate-link, p: 5'-phosphate, annealed according to and modified after Kozarewa et al. (Kozarewa et al., 2009), size-selection of fragments with linkers ligated to both ends and Q-PCR-based quantification as described above.

High-throughput sequencing

DNA from chromatin immunoprecipitation (10-50 ng) was adapter-ligated and PCR amplified according to the manufacturer's protocol (Illumina, San Diego, USA). ChIP fragments were sequenced for 36 cycles on an Illumina Genome Analyzer according to the manufacturer's instructions. The first 23-25 bp for each sequence tag returned by the Illumina Pipeline was aligned to the mm8 assembly (NCBI Build 36) using ELAND allowing up to 2 mismatches. Only tags that mapped uniquely to the genome were considered for further analysis. ChIP-Seq experiments where visualized by preparing custom tracks for the UCSC Genome browser in a manner similar to that previously described (Robertson et al., 2007). All public data used in this study was also remapped from raw sequence data to ensure consistent data handling across samples.

ChIP-Seq Peak and DNA Sequence analysis

Data analysis was performed using HOMER, a software suite for ChIP-Seq analysis and created in part to support this study. The methods described below have been implemented and are freely available at http://biowhat.ucsd.edu/homer/.

ChIP-Seq quality control

The ChIP-Seq sequence data was checked for abnormal GC content, excessive clonal amplification (multiple tags starting at the same genomic position), inherent sequence bias in the sequenced tags and surrounding genomic positions and contamination with plasmid/cDNA sequences. Experiments that exhibited aberrant GC content compared to the mouse genome, excessive clonal amplification (>25%) or an inherent sequence bias were repeated, tags derived from plasmids/cDNA were removed from the data sets.

Identification of ChIP-Seq peaks.

The identification of ChIP-Seq peaks (bound regions) was performed using a custom approach (HOMER) that combines features of previously published methods (Robertson et al., 2007; Zhang et al., 2008). For each ChIP-Seq experiment, ChIP-enriched regions (peaks) were found by first identifying significant clusters of ChIP-Seq tags and then filtering these clusters for those significantly enriched relative to background sequencing and local ChIP-Seq signal. First, we centered raw ChIP-Seq tags representing the edge of ChIP fragments by 75 bp to mark the approximate center of fragments isolated in the ChIP experiment. We considered one tag from each unique position to eliminate peaks resulting from clonal amplification of fragments that can arise during library preparation and cluster generation steps in the ChIP-Seq protocol. Putative peaks were then identified by searching for clusters of tags within a sliding window of 200 bp. Putative peaks were then filtered based on the following 4

conditions. (1) The number of tags in each cluster must exceed a threshold corresponding to a false discovery rate of 0.1% based on the assumption that randomly distributed tags would naturally form clusters given the large number of tags sequenced. This threshold was empirically calculated by randomizing tag positions and repeating the tag clustering procedure to determine the expected number of clusters exceeding each tag threshold. (2) Adjacent peaks must be greater then 500 bp away from one another. (3) Peaks must have at least 4-fold more tags (normalized to total tag count) than the input control sample from the same cell type to eliminate background artefacts. (4) Peaks must have 4-fold more tags per bp in the peak region (200 bp) relative to the surrounding region (10 kb) to avoid identifying regions with genomic duplications or peaks without localized binding. In the case of BLRP-ChIP for biotin tagged LXRβ, a BLRP-ChIP in cells expressing only the biotin ligase but no BLRP-tagged transcription factor was used as a negative control. In addition, this BLRP-LXRβ experiment contained vector sequences for several cDNA-containing plasmids used in the laboratory. To remove this erroneous signal, peaks located on exons in the BLRP-LXRβ experiment were removed for further analysis. Peaks in the public data used in this study were identified in an identical manner, to keep the analysis consistent between datasets. Overall, the peaks identified using HOMER were qualitatively similar to those identified using other methods. For example, 89% of peaks identified using MACS (Zhang et al., 2008) for PU.1 were also identified using HOMER with comparable numbers of peaks found with both methods.. Peaks were associated with genes by identifying the nearest RefSeq TSS.

Identification of ChIP-Seq H3K4me1 Enhancer Regions.

H3K4me1 is commonly found enriched several hundred bp around transcription factor binding regions, but in some cases it can be found spread over vast regions or at promoters without apparent association with transcription factor-bound sites. To distinguish between these two cases, we modified our peak finding parameters to find clusters of tags within a 1 kb window, as opposed to 200 bp for transcription factors. We still required the peak region to have 4-fold more tags (normalized to total count) than input sample from the same cell type. We also required the peaks to contain 4-fold more tags per bp in the 1 kb peak region relative to the surrounding 10 kb region to ensure the peaks are 'focal', increasing our chances that they contain regulatory elements within the 1 kb region and not in adjacent regions. In addition, H3K4me1 is often associated with promoter regions where H3K4 methylation undergoes a gradual loss from H3K4me3 near the TSS to H3K4me2 from 0.5-1 kb from the TSS and then H3K4me1 from 1-2 kb from the TSS. We found this region to be relatively devoid of enriched motifs since H3K4 methylation in this region is likely an indiscriminate consequence of processes originating at the promoter. To enrich for H3K4me1 peaks that are enhancers, we removed H3K4me1 peaks that contained significant numbers of H3K4me3 tags (>0.5x the number of H3K4me1 tags) within 3 kb of the H3K4me1 peak, in addition to eliminating peaks found within 3 kb of an annotated TSS.

Due to the restrictive conditions placed on H3K4me1 focal peak identification, many transcription factors with high H3K4me1 tag density in their vicinity may not be near a "focal" H3K4me1 peak. To assess if individual transcription factor–bound regions such as PU.1 peaks were considered marked by H3K4me1, the total number of H3K4me1 ChIP-Seq tags found within 1 kb of the transcription factor binding site was calculated. If this tag count exceeded the minimum number of tags used to determine H3K4me1

peaks, the binding site was considered "marked" by H3K4me1. This same procedure was also used to determine peaks marked by H3K4me3.

Comparison of ChIP-Seq experiments using scatter plots and histograms.

To facilitate the comparison of ChIP-Seq tag densities between different sequencing libraries, all ChIP-Seq experiments were normalized by the total number of mapped tags in each experiment such that the normalized tag counts totalled 10^7. When comparing peaks from different experiments, peak regions were considered co-bound by both factors if peak positions from each experiment located within 100 bp of one another, unless specifically noted. ChIP-Seq scatter plots were created by considering the number of normalized ChIP-Seq tags located in the vicinity of peaks across multiple experiments (i.e. Figure 1C). First, a set of genomic positions corresponding to the combined peak positions of the two experiments to be compared is defined to represent each data point in the scatter plot. In the case where multiple sets of peaks are used (i.e. macrophage and B cell PU.1 peaks), adjacent peaks within 100 bp of each other from different sets are condensed into a single peak position represented by the average of their genomic positions. For each peak position, the number of normalized ChIP-Seq tags positioned within 200 bp of the center of the peak are counted for each experiment to be compared. This can be repeated for any number of ChIP-Seq experiments in order to cross-reference their results. The scatter plots are then created by calculating the $\log_2$ of the tag counts from two experiments and plotting these values as (x,y) coordinates. For H3K4me1 peaks, peaks were merged when found within 500 bp of each other, and normalized ChIP-Seq tags where counted within 500 bp of the center of a given H3K4me1 genomic peak position. Histograms of tag densities (such as H3K4me1) were calculated using position corrected, normalized tags.

Description of HOMER for *de novo* motif discovery

Motif discovery was performed using a comparative algorithm similar to those previously described (Linhart et al., 2008) and an in depth description will be published elsewhere (Benner et al., in preparation). Briefly, sequences were divided into target and background sets for each application of the algorithm (Choice of target and background sequences are noted below). Background sequences were then selectively weighted to equalize the distributions of CpG content in target and background sequences to avoid comparing sequences of different general sequence content. Motifs of length 8, 10, and 12 bp were identified separately by first exhaustively screening all possible oligos for enrichment in the target set compared to the background set by assessing the number of target and background sequences containing each oligo and then using the cumulative hypergeometric distribution to score enrichment. Up to two mismatches were allowed in each oligonucleotide sequence to increase the sensitivity of the method. The top 200 oligonucleotides of each length with the best enrichment scores were then converted into basic probability matrices for further optimization. HOMER then generates motifs comprised of a position-weight matrix and detection threshold by empirically adjusting motif parameters to maximize the enrichment of motif instances in target sequences versus background sequences using the cumulative hypergeometric distribution as a scoring function. Probability matrix optimization follows a local hill-climbing approach that weights the contributions of individual oligos recognized by the motif to improve enrichment, while optimization of motif detection thresholds were performed by exhaustively screening degeneracy levels for maximal enrichment during each iteration of the algorithm. Once a motif is optimized, the individual oligos recognized by the motif are removed from the data set to facilitate the identification of

additional motifs. Sequence logos were generated using WebLOGO (http://weblogo.berkeley.edu/). Known motif enrichment was performed by identifying instances of each motif in the target and background sequences and scoring enrichment using the cumulative hypergeometric distribution. Known motifs were derived from JASPAR and their detection thresholds were determined using an exhaustive array of public high-quality ChIP-Seq and ChIP-chip experiments. Motifs for which no high-throughput data exists were discarded for this analysis.

Analysis of ChIP-Seq Peaks for *de novo* motif enrichment

Two general strategies were employed when using HOMER to analyze ChIP-Seq peaks for enriched motifs. For the first strategy, peak sequences (+/- 100 bp for transcription factors, +/- 500 bp for H3K4me1 peaks) are compared to 50,000 randomly selected genomic fragments of the same size, matched for CpG% to remove sequence bias introduced by CpG Islands. This enables HOMER to identify motifs that are generally enriched in ChIP-Seq peaks versus the genomic background. The second strategy used was to compare peak sequences to a set of defined background sequences. This strategy can be useful for identifying motifs that are specifically enriched in a subset of ChIP-Seq peaks. For example, if distal macrophage-specific PU.1 peaks are analyzed using distal B cell-specific PU.1 peaks as a background, enrichment for the consensus PU.1 motif is eliminated while macrophage-specific motifs such as AP-1 and C/EBP become highly enriched. By default the first strategy is used, unless a specific background is noted within the text.

Cloning and plasmid preparation

For cloning of PU.1 enhancer assay plasmids we used Primer3 software (Rozen and Skaletsky, 2000) to design primers by inputting 300-600 bp of sequence crosslinked by

PU.1. Each primer pair was required to flank the peak of PU.1 tags and to include at least 150 bp on each side of the peak. To the 5′ end of each primer, we added 15 bp tails homologous to the vector cloning site to facilitate cloning by the Infusion Cloning System (Clontech cat. no. 639605) (left primer tail: 5'- TCTTACGCGTGCTAGC -3'; right primer tail: 5'- TATCGAAGATCTCGAG -3'). We amplified the fragments using the touchdown PCR protocol previously described (Trinklein et al., 2004) and Titanium Taq Enzyme (Clontech, cat. no 639210). To clone our PCR-amplified fragments using the In-Fusion Cloning System (Clontech), we combined 2 µl of purified PCR product and 100 ng of linearized pGL3-TATA-IIB vector. The pGL3-TATA-IIB constructs contain a wild type octamer site (bold) inserted 10 base pairs upstream of the TATA box of a minimal Vκ promoter (−32 to +25) (Bertolino and Singh, 2002) flanked by an optimal TFIIB binding site (underlined): TA**ATTTGCAT**ACCGACTTCTTTATATAAGGGCGCC. We added this mixture to the infusion reagent and incubated at 37°C for 15 min followed by 15 min incubation at 50°C. The iNOS control enhancer (-209 to -48) and immunoglobulin enhancers were previously described (Alley et al., 1995; Andersson et al., 2000; Meyer et al., 1990). After incubation, the mixture was diluted and transformed into competent cells (Clontech cat. No. 636758). Minipreps of clones were performed using an automated robotic platform (Tecan, Freedom EVO200) and Nucleospin Robot-96 plasmid kit (Clontech cat. No. 636797). We screened clones for insert by restriction enzyme cutting and larger cultures of positive clones were prepared. We quantified DNA with a 96 well multi-detection microplate reader (Tecan, Sapphire II) and standardized concentrations to 500 ng/µL for transfections.

For construction of LXR enhancer assay plasmids Primer3 software (Rozen and Skaletsky, 2000) was used to design primers by inputting 800-1400 bp of sequence centred on LXRβ binding sites. Each primer pair was designed so that the resulting amplicon included the LXRβ binding site and flanking sequence demarcated by focal H3K4me1. To facilitate cloning into the pGL4 vector (Promega) sequences corresponding to recognition sites for KpnI (5'-GGTACC) and BglII (5'-AGATCT) were added to the 5′ end of sense and antisense primers respectively. We amplified the fragments using the touchdown PCR protocol previously described (Trinklein et al., 2004) and DNA Phusion polymerase (New England Biolabs). KpnI/BglII-digested fragments were cloned into the linearized pGL4-TATA-TK vector 19 bp upstream of a minimal TK promoter using T4 DNA ligase (Enzymatics). The pGL4-TATA-TK is the pGL4.10 luciferase reporter plasmid (Clontech) modified by inserting the minimal TATA-containing thymidine kinase (TK) promoter (-119/+25) from pTAL 34 bp upstream of the luciferase coding region. Clones were screened for insert by restriction enzyme and sequencing analyses, then large cultures of positive clones were prepared using PureLink HiPure Plasmid Maxiprep Kit (Invitrogen). DNA quantitation was performed with a 96 well multi-detection microplate reader (μQuant, BioTek instruments Inc.) and standardized concentrations to 400 ng/μL for transfections. Primer sequences for cloning enhancer fragments provided upon request.

Reporter gene activity assays

For PU.1 enhancer assay experiments (Figure S6A), we performed transfections of primary peritoneal macrophages or primary splenic B (treated with 100 ng/ml LPS for 24 h to induce a mitogenic response) using a 96 well Amaxa shuttle integrated in a Tecan, Freedom EVO200 liquid handler. We electroporated 500 ng of experimental

firefly luciferase plasmid with 100 ng of Renilla luciferase control plasmid (pRL-CMV, Promega cat. no. E2261) in duplicate, using the Amaxa shuttle according to the manufacturer's recommendation. We seeded 200,000 per well in 96 well tissue culture plates. Cells were lysed 18-24 hr post-transfection, depending on cell type. We measured firefly luciferase and Renilla luciferase activity using a Berthold *Microlumatplus* Luminometer and the Dual Luciferase Kit (Promega, cat. no. E1960) according to the protocol suggested by the manufacturer. Data from primary cells are given as a transformed ratio of firefly luciferase to Renilla luciferase. We determined the mean ratio of three or four independent experiments performed in duplicate.

For all other reporter assays, transfection of the indicated mouse cell lines was achieved using Superfect reagent (Qiagen) according to manufacturer's recommendation. BIRA-RAW264.7 stable cells were cotransfected with 400 ng ABCA1 promoter-driven firefly luciferase expression plasmid and 200 ng pCMV (Promega), pCMV-LXRβ, or BLRP-LXRβ. For LXR enhancer experiments, RAW264.7 cells were cotransfected with 400 ng experimental firefly luciferase expression plasmid and 200 ng pCMV-LXRβ. Cells were seeded at 125,000 cells per well in 48-well tissue culture plates. At 24 hr post-transfection cells were treated with either DMSO or 1 μM GW3965 (provided by GlaxoSmithKline) for 24 hr. Cells were lysed and firefly luciferase activity was measured using a Veritas microplate luminometer (Turner Biosystems) according to manufacturer's protocol. A β-galactosidase expression vector was cotransfected (20 ng/well) as an internal control. Relative light units (RLU) were given as transformed ratio of firefly luciferase to β-galactosidase. Values are the mean ratio of three independent experiments performed in triplicate.

Generation of biotin-tagged LXRβ for ChIP-Seq analysis

Due to lack of antibodies providing sufficient ChIP enrichment of LXRs on known target genes in macrophages, we implemented and validated an *in vivo* biotin tagging strategy (de Boer et al., 2003; Mito et al., 2005). To generate biotin-tagged LXRβ for ChIP-Seq analysis, an expression vector was constructed in which a double stranded oligonucleotide encoding the amino acid sequence MAGGLNDIFEAQKIEWHEDTGGGGSGGGGSGENLYFQS was fused in frame with the LXRβ initiator methionine. Amino acids 1-20 represent a biotin ligase recognition peptide (BLRP), in which the lysine residue at position 13 is a substrate for the bacterial biotin ligase (BirA). The glycine-rich stretch following the BLRP sequence provides a spacer region, and the ENLYFQS sequence provides a specific cleavage site for TEV protease (Invitrogen). BLRP-LXRβ was placed under the control of the CMV early region enhancer/chicken β actin promoter in a plasmid conferring puromycin resistance. BLRP-tagged LXRβ was shown to exhibit ligand-dependent transcriptional activity comparable to WT-LXRβ in transient transfection assays (see Supplemental Fig. 13). The BLRP-LXRβ expression plasmid was then transfected into RAW264.7 macrophages engineered to stably express BirA (BIRA-RAW264.7 stable cell line). Multiple stable cell lines were isolated and screened for LXRβ expression and BLRP-LXRβ biotinylation via western blot using anti Avi-tag antibody specifically recognizing the BLRP tag (Genscript) or HRP-streptavidin (Jackson Immunoresearch). Functional validation of verified BLRP-LXRβ RAW264.7 stable lines was performed by monitoring GW3965 response in both transient transfection (Figure S5A) and quantitative transcript analysis of the LXR target gene ABCA1. ChIP-Seq analysis was

performed following standard protocols, except that crosslinked protein DNA adducts were purified using Nanolink Streptavidin Magnetic Microspheres (Solulink), and LXRβ-DNA adducts were specifically eluted following TEV cleavage (AcTEV, Invitrogen). ChIP-Seq results presented in these studies utilized a cell line in which BLRP-LXRβ expression levels were approximately 2-fold higher than the endogenous LXRβ levels in the parental RAW264.7 cell line, and about two third of the level of endogenous LXRβ observed in thioglycolate-elicited primary macrophages (Figure S5B). Qualitatively similar results were obtained for several other cell lines expressing higher levels of BLRP-LXRβ with respect to localization at LXR target genes, enrichment of LXRE motifs, and co-enrichment of PU.1 and AP-1 motifs, although a larger total number of peaks were identified.

RNA isolation and quantitative RT-PCR analysis

Total RNA from PU.1-ER cells, RAW264.7 cells, BLRP-LXRβ RAW264.7 cells, thioglycollate-elicited peritoneal macrophages and bone marrow derived macrophages was prepared using RNeasy kit (Qiagen). One μg of total RNA was used for cDNA synthesis via SuperScript III First Strand Kit (Invitrogen), and 1 μl of cDNA was used for real time PCR using gene-specific primers (primer sequences below). Quantitative transcript (SYBR GreenER) analysis was performed on an Applied Biosystems 7300 Real-time PCR system using SYBR GreenER qpcr mastermix (Invitrogen). Values are normalized for 36B4 content.

Western Blot

Nuclear extracts were prepared from BLRP-LXRβ RAW 264.7 cells using a commercial kit (NE-PER, Pierce). For assessment of BLRP-LXRβ expression and biotinylation levels, nuclear extracts were resolved by SDS–PAGE and immunoblotted

using anti-Avitag antibody (cat#A00674, GenScript) and HRP-Streptavidin (cat#016-030-084, Jackson Immunoresearch) antibodies respectively. Western blots were visualized using Supersignal West Pico Chemiluminescent Substrate (Thermo Scientific) and Blue X-Ray Film (Phenix Research Products).

Sequences of oligonucleotides used for ChIP-qPCR

Sequence Description	Sequence
ABCA1 distal sense	GCCCCGCCCTCCCTATTCGT
ABCA1 distal antisense	ACAGTCACATGGCGGCTGGA
ABCA1 intron sense	GCGTTCGCTCTCCCACCTGC
ABCA1 intron antisense	AGCTGGGGCTTAGAGAGGGCA
ABCG1 sense	GGCACACTCCCAGCTCTGTCC
ABCG1 antisense	CCGCCACCCACCACACTGAG
AB124611 sense	CAGGAGTCTCTTTTGGTGCC
AB124611 antisense	GGCATCTCTCCTCCCATGTA
ACSL3 sense	AAGGGCTCAATCCCCGCCCT
ACSL3 antisense	GGGCTGGCGCTCGTTGCATA
APOE sense	CCTCCCTGCCCCCTCCTTCC
APOE antisense	AGCTGCCAGGGGGTCACTGT
BCL2L1 sense	GACCAACATCCCTCAGGAAA
BCL2L1 antisense	CCGGAAGCATAAGAGGATGA
CSF2RB2 sense	TCCGTATCAGGAAGCCACTT
CSF2RB2 antisense	GCACTGGCAACTTCCTCAAT
ELOVL5 sense	AACAGGAAGTGACGAAGGGA
ELOVL5 antisense	CCATGCAGCTCATTGGTACA
GRAMD1B sense	AGACCGTGCAGCTTTCAACT
GRAMD1B antisense	CTGGGGTTACTGCAGGACAT
IgKappa sense	GCAACTGTCATAGCTACCGTCAC
IgKappa antisense	GTGTATGAGGCTTTGGAAACTTGA
LIPN sense	TGGATTGCAGCTCAACTGAC
LIPN antisense	AAATGGGGAAGCAGACTGTG
LPCAT3 sense	GGGCTCCCCCAGAGCCTTCA
LPCAT3 antisense	CTGCTGTCACCCCACGAGCG
NDRG1 sense	AGAGGGAGACGAAGATGGGT
NDRG1 antisense	CGCCTATAAAATCGCCCTAC
PMP22 sense	TATGCCGCTCCTGGCTCCCC
PMP22 antisense	CTTGGGGACAGCGCCTGTGG
PNPO sense	GGGCAGGGATCCCCTCCTGG
PNPO antisense	CAGCACCTGCCCTGCGGTTT
SCD1 sense	AAAGTGCGCACGCACCTCCA
SCD1 antisense	TGCGGACACCCAGAGAGGCA
SCD2 sense	CTCCCACATAAGGAAGCTGG
SCD2 antisense	GTGCTGACCGAGAGTAACCC
SREBP1 sense	GCTCGGGTTTCTCCCGGTGC
SREBP1 antisense	TGGGACGACAGTGACCGCCA

Sequences of oligonucleotides used for qRT-PCR

Sequence Description	Sequence
ABCA1 sense	AAAACCGCAGACATCCTTCAG
ABCA1 antisense	CATACCGAAACTCGTTCACCC
ABCG1 sense	CCGGATTCTTTGTCAGCTTT
ABCG1 antisense	AGCCGTAGATGGACAGGATG
APOC1 sense	TTCATCGCTCTTCCTGTCCT
APOC1 antisense	CCGGTATGCTCTCCAATGTT
APOE sense	AACCGCTTCTGGGATTACCT
APOE antisense	GCTGTTCCTCCAGCTCCTTT
ACSL3 sense	GCTGGGCTCAGATCAACTTC
ACSL3 antisense	AGAGGATGATGCAGAGGTGG
ARL4C sense	GCCGAGATTGAGAAGCAACT
ARL4C antisense	GAGACTTCCTGCGTTTCAGG
BCL2L1 sense	GCTGGGACACTTTTGTGGAT
BCL2L1 antisense	TGTCTGGTCACTTCCGACTG
CSF2RB2 sense	CTATGGATGTGCAGTGTGGG
CSF2RB2 antisense	CGGATCTCCAGGAGTGACAT
ELOVL5 sense	ATACATGAAGAACCGGCAGC
ELOVL5 antisense	TGTATTTGCCTTCCCACACA
GRAMD1B sense	TCCATTGAGATTACGCCCTC
GRAMD1B antisense	CTCAGGAACCTGCTCGAATC
LIPN sense	CGACTGGATGTGTACATGGC
LIPN antisense	CAAATGGCAGTGGGTACCTT
LPL sense	GCCCAGCAACATTATCCAGT
LPL antisense	GTCAGACTTCCTGCTACGCC
LXRβ sense	GCGTGTGCGGAGACAAGGCT
LXRβ antisense	CGCTGCCCCGACAGGCATAG
NDRG1 sense	CAAGAGTGTCATTGGCATGG
NDRG1 antisense	AGGGGTTCACATTCATGAGC
PLTP sense	CCAAGATCTGCTGCTGAACA
PLTP antisense	AGACCTGTTCGGATGGACAC
SCD1 sense	GCGATACACTCTGGTGCTCA
SCD1 antisense	CTGGCAGAGTAGTCGAAGGG
SCD2 sense	GCTCTCGGGAGAACATCTTG
SCD2 antisense	CAGCCCTGGACACTCTCTTC
36B4 sense	agggcgacctggaagtcc
36B4 antisense	cccacaatgaagcattttgga

Supplemental References

Alley, E.W., Murphy, W.J., and Russell, S.W. (1995). A classical enhancer element responsive to both lipopolysaccharide and interferon-gamma augments induction of the iNOS gene in mouse macrophages. Gene *158*, 247-251.

Andersson, T., Samuelsson, A., Matthias, P., and Pettersson, S. (2000). The lymphoid-specific cofactor OBF-1 is essential for the expression of a V(H) promoter/HS1,2 enhancer-linked transgene in late B cell development. Mol Immunol *37*, 889-899.

Bertolino, E., and Singh, H. (2002). POU/TBP cooperativity: a mechanism for enhancer action from a distance. Mol Cell *10*, 397-407.

de Boer, E., Rodriguez, P., Bonte, E., Krijgsveld, J., Katsantoni, E., Heck, A., Grosveld, F., and Strouboulis, J. (2003). Efficient biotinylation and single-step purification of tagged transcription factors in mammalian cells and transgenic mice. Proc Natl Acad Sci U S A *100*, 7480-7485.

Decker, T., Pasca di Magliano, M., McManus, S., Sun, Q., Bonifer, C., Tagoh, H., and Busslinger, M. (2009). Stepwise activation of enhancer and promoter regions of the B cell commitment gene Pax5 in early lymphopoiesis. Immunity *30*, 508-520.

Kozarewa, I., Ning, Z., Quail, M.A., Sanders, M.J., Berriman, M., and Turner, D.J. (2009). Amplification-free Illumina sequencing-library preparation facilitates improved mapping and assembly of (G+C)-biased genomes. Nat Methods *6*, 291-295.

Linhart, C., Halperin, Y., and Shamir, R. (2008). Transcription factor and microRNA motif discovery: the Amadeus platform and a compendium of metazoan target sets. Genome Res *18*, 1180-1189.

Meyer, K.B., Sharpe, M.J., Surani, M.A., and Neuberger, M.S. (1990). The importance of the 3'-enhancer region in immunoglobulin kappa gene expression. Nucleic Acids Res *18*, 5609-5615.

Mito, Y., Henikoff, J.G., and Henikoff, S. (2005). Genome-scale profiling of histone H3.3 replacement patterns. Nat Genet *37*, 1090-1097.

Pan, Z., Hetherington, C.J., and Zhang, D.E. (1999). CCAAT/enhancer-binding protein activates the CD14 promoter and mediates transforming growth factor beta signaling in monocyte development. J Biol Chem *274*, 23242-23248.

Robertson, G., Hirst, M., Bainbridge, M., Bilenky, M., Zhao, Y., Zeng, T., Euskirchen, G., Bernier, B., Varhol, R., Delaney, A., *et al.* (2007). Genome-wide profiles of STAT1 DNA association using chromatin immunoprecipitation and massively parallel sequencing. Nat Methods *4*, 651-657.

Rozen, S., and Skaletsky, H. (2000). Primer3 on the WWW for general users and for biologist programmers. Methods Mol Biol *132*, 365-386.

Trinklein, N.D., Aldred, S.F., Hartman, S.J., Schroeder, D.I., Otillar, R.P., and Myers, R.M. (2004). An abundance of bidirectional promoters in the human genome. Genome Res *14*, 62-66.

Wilson, D., Charoensawan, V., Kummerfeld, S.K., and Teichmann, S.A. (2008). DBD--taxonomically broad transcription factor predictions: new content and functionality. Nucleic Acids Res *36*, D88-92.

Wu, C., Orozco, C., Boyer, J., Leglise, M., Goodale, J., Batalov, S., Hodge, C.L., Haase, J., Janes, J., Huss, J.W., 3rd, *et al.* (2009). BioGPS: an extensible and customizable portal for querying and organizing gene annotation resources. Genome Biol *10*, R130.

Zhang, Y., Liu, T., Meyer, C.A., Eeckhoute, J., Johnson, D.S., Bernstein, B.E., Nussbaum, C., Myers, R.M., Brown, M., Li, W., *et al.* (2008). Model-based analysis of ChIP-Seq (MACS). Genome Biol *9*, R137.